First-principles study of ternary hydrides for solid state hydrogen storage

Joachim Scheerlinck*[1], Ian Lesnik[2], Thibaut D'homme†[3], and Jie Huang‡[4]

[1,2] *Department of Physics, Ghent University, Ghent, Belgium*
[3] *Department of Physics, UAntwerpen, Antwerpen, Belgium*
[4] *Department of Applied Physics, Aalto University, Helsinki, Finland*

(Dated: December 10, 2023)

Solid state storage of hydrogen is a promising step for the ongoing energy transition. In this paper, we perform first-principles calculations on a selection of crystals using Quantum Espresso. The selection of crystals consists of ternary hydrides containing an alkali metal and aluminum (AM-Al-H), with some additional calculations for Li-B-H. The selection of structures is made, based on convex hull crystals of the Na-Al-H category ternary phase diagram with AlH_3 and NaH as endmembers. Based on our calculations, the most suitable ternary hydrides are found to be Li_3AlH_6 and $LiBH_4$ mainly based on hydrogen density, weight percentage and formation energies of endmembers. The post-processing codes can be found in this GitHub repository MS_Project https://github.com/HuangJiaLian/MS_Project.

Keywords: hydrogen storage, density functional theory

I. Introduction

Hydrogen as an energy carrier is very interesting because of its (potentially) non-polluting nature and high energy per mass (almost 3x more than diesel [1]). However, its storage remains one of the critical problems that prohibit the implementation [2]. Under standard conditions, a liter of hydrogen gas will only provide around 0.003 kWh while the same volume of diesel holds around 3 kWh [1].

By thinking of the ideal gas law, it is easy to see that increasing the pressure or lowering the temperature will also increase the volumetric density. However, the safety of storing a flammable gas under high pressure is concerning regarding safety [3, 4] and liquification of hydrogen is generally not economic [3]. These factors make it interesting to research solid state storage. The focus of this paper is mainly on ternary hydrides containing an alkali metal and aluminum, based on Na-Al-H structures. Additionally, crystals of the form Li-B-H were studied. In section II. of this paper, our methods for choosing suitable crystals are explained, and the technical data of the calculations is given. Next, in section III., the results are shown and discussed. At last, the content of this paper is summarized in section IV..

II. Methods and Material

Density functional theory (DFT) [5, 6] calculations were conducted using Quantum Espresso (QE) [7, 8] with Perdew-Burke-Ernzerhof (PBE) exchange correlation functional [9] for generalized gradient approximation (GGA). The standard solid-state pseudopotentials (SSSP) library (PBE Efficiency v1.3.0) [10] was used. The Atomic Simulation Environment (ASE) [11, 12] and pymatgen [13] are used to process the CIF files. The bilbao website [14–16] is used to determine the degree of freedom. The basis set size for the wave functions (ecutwfc), the basis set size for the density (ecutrho), and the K-points in reciprocal space were determined by convergence testing using the minimum precision of 3 mRy/au in forces and 3 kbar for any component of the stress tensor as the criteria.

The following types of ternary hydrides were investigated: XH, $XAlH_4$, X_3AlH_6, $X_5Al_3H_{14}$ and AlH_3, with X being one of the following alkali metals: Li, Na, K, Rb or Cs. Appart from these crystals, to broaden the scope of this project, the LiB hydrides were also investigated. These were added because we wanted an interesting extension and B is very similar to Al in the periodic system. Due to the time constraint of this project, only one family containing B could be tested, so we decided to pair it to Li, the most promising alkalimetal from the previously stated groups. As an example, the Na containing hydrides are shown in their respective phase diagram in figure 1, retrieved from the Materials Project. The QE input files of the crystals were generated using cif2cell [17], based on the CIF files downloaded from the Materials Project [18]. For a given crystal there might be multiple CIF files available on the Materials Project. Therefore only the crystals with the lowest energy above convex hull prediction were used.

*Joachim.Scheerlinck@UGent.be
†thibaut.dhomme@student.uantwerpen.be
‡jie.huang@aalto.fi

Our approach involved a systematic investigation of each category of aluminum-containing alkali hydrides. Utilizing CIF files, we extracted fundamental data such as the number of atoms, geometrical degrees of freedom, hydrogen pair density, and hydrogen pressure. The initial two parameters played a significant role in accelerating the convergence testing process, with the third parameter serving as a crucial criterion for evaluating the efficacy of hydrogen storage under ideal conditions. The fourth parameter was used for comparative analysis with pressurized hydrogen gas storage systems. Specifically, the selection of the structure with the minimum number of atoms and geometrical degrees of freedom within each category facilitated efficient convergence testing. The results obtained from this testing were subsequently applied to all other structures within the same category, speeding up the overall workflow. Furthermore, these settings were used in the relaxation simulations as to create phase diagrams for every category of crystals. These phase diagrams are created in order to indicate the stability of these crystals. In the case where the formation energy of a crystal is too high (above the convex hull), it can spontaneously decompose into more stable crystals. The following generalized endmember decomposition, where X is one of the alkali metals were used for the phase diagrams:

$$(X)AlH_4 \longrightarrow AlH_3 + (X)H \tag{1}$$

$$(X)_5Al_3H_{14} \longrightarrow 3\,AlH_3 + 5\,(X)H \tag{2}$$

$$(X)_3AlH_6 \longrightarrow AlH_3 + 3\,(X)H \tag{3}$$

Note that, for the Li category of crystals the same decomposition is true for Al as well as B. It should also be noted, as previously mentioned, for every category, distinguishable by their different alkali elements, the same 4 types of crystal are used. However, not every category of crystals has those 4 types of crystal. If one or more crystals were missing, the corresponding Na type crystal was used (for all available symmetries) with the Na atoms replaced by the alkali element specific to that category. Examples will be given in the following section.

When choosing suitable crystals for hydrogen storage, it is important to establish some criteria. We are interested in increasing the volumetric density so this would be a logical first criterium. Also, as explained in the section I., the energy density per mass is a big strength of hydrogen. This will be lowered with storage in crystals so a good contender would ideally have a high weight percentage. Concretely, based on [2], we choose to put the lower limit at 9 percent.

Further, we want it to be efficient at ab- and desorption of hydrogen for the storage system to remain adequately efficient. If a large amount of energy is needed for the extraction, it wouldn't be efficient enough for real implementations. For this, we want the crystals to have formation energies on the convex hull for stability, but as close as possible to zero. In other words, there should be stability, but not so much that it hinders the application. Note that we use the formation energy

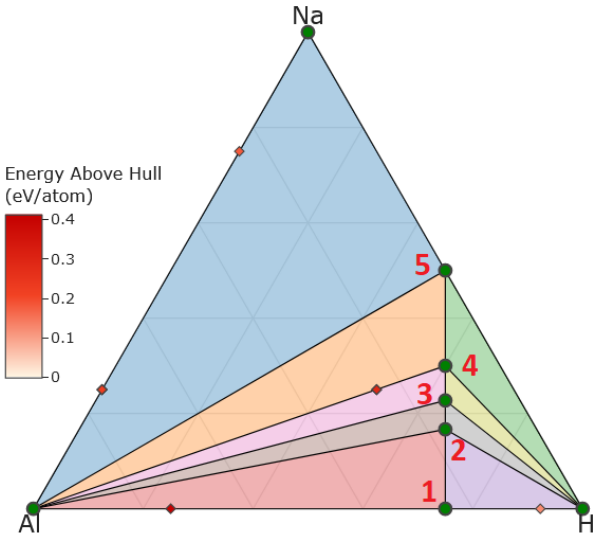

Figure 1: Ternary phase diagram for Al, Na and H, where (1) to (5) represent AlH_3, $NaAlH_4$, $Na_5Al_3H_{14}$, Na_3AlH_6 and NaH respectively. [18]

with respect to the endmembers. This gives us only an indication as opposed to a verification of the criterium. This is something we have to deal with since more complex methods (that take the exact reaction paths into account) are out of the scope of this project.

III. Results and Discussion

A. Preliminary calculations

Our investigation of alkali hydrides begins with the collection of sodium crystals, NaH, $NaAlH_4$, Na_3AlH_6, $Na_5Al_3H_{14}$, and the endmember, AlH_3. We gathered data for the number of atoms in the conventional cells of each crystal as well as their geometric degrees of freedom. The number of hydrogen atoms in the conventional cells relative to its size (as given from the CIF files) then determines the density of hydrogen and the pressure needed to obtain that density of hydrogen as a gas using the ideal gas law. For the purposes of this study, the ideal gas law gives a good approximation for the pressure. For the result of these properties, we refer to table 6 in the Appendix. This analysis was then repeated for each of the other alkali hydrides.

B. Convergence test

For the convergence test, $NaAlH_4$ is used as the representative for the crystal group Na-Al-H because it both has a low number of degrees of freedom (high symmetry) and also a small number of atoms. The energies and forces of each atom converged at the $5 \times 5 \times 5$ k-mesh. The choice was made to continue with a $7 \times 7 \times 7$ k-mesh, motivated by the higher accuracy and the reasonable increase in computational cost. We could have also chosen a non-symmetrical k-mesh (e.g. $5 \times 5 \times 3$), since this represents the ratio between the lattice parameters better. However, we have access to sufficient computing resources and since the same parameters are used for the endmembers (which are cubic), it made more sense to keep the

Crystal group	k-mesh	ecutwfc	ecutrho
Li-Al-H	$5 \times 5 \times 5$	70	200
Na-Al-H	$7 \times 7 \times 7$	70	280
K-Al-H	$15 \times 15 \times 15$	60	240
Rb-Al-H	$5 \times 5 \times 5$	50	250
Cs-Al-H	$7 \times 7 \times 7$	80	400
Li-B-H	$7 \times 7 \times 7$	150	600

Table 1: The convergence test results for each crystal group.

k-mesh symmetrical.

Subsequently, the wave function cutoff was tested. We held a constant multiplication factor of 5 between ecutwfc and ecutrho. We tested different values in steps of 10 for the ecutwfc. We observed sufficient convergence at ecutwfc = 70. We kept the 7x7x7 k-mesh and ecutwfc = 70 and varied the multiplication factor. Here it was found that a factor of 4 adequate convergence). The general convergence testing results are given in Table 1.

C. Structure relaxation results and hydrogen density

After retrieving the above settings, these were used in the relaxation simulations for the atomic position and cell shape. From these simulations, the H_2 densities, weight percentages (of the hydrogen) and ideal gas equivalent pressures were calculated. The results are shown in Table 2, together with the number of atoms and the space group. As written in section II., for hydrogen storage, both high H_2 density and weight percentage are desirable. Using this criterion exclusively, the Li-B-H and Li-Al-H category crystals make the best hydrogen storage materials. It also becomes clear that if the same amount of hydrogen gas were to be stored without the use of crystals, the pressure would be very high.

More specifically, still purely based on these criteria, the most interesting ternary hydrides are the ones in the Li-B-H and Li-Al-H families. All the others don't have adequate weight percentages. The binary hydrides AlH_3, LiH and BH_3 are also interesting, but we can't apply the other criteria on them since they themselves are the reference energies. With the unknown reaction paths for hydrogen desorption, this is a limitation we have to deal with for this study.

D. Formation energies

The next essential criterion that is investigated is the stability of the crystals. To this end, the phase diagrams of X-Al-H category crystals are shown in Figure 2. The formation energies of these crystals are shown in Table 3. From the Li-Al-H phase diagram, Figure 2(a) it becomes clear that $LiAlH_4$ and $Li_5Al_3H_{14}$ are unstable and therefore not wanted for hydrogen storage. In general, all crystals of the form $X_5Al_3H_{14}$ are unstable, except for $Na_5Al_3H_{14}$. However, this could be due to the lack of CIF files in the databases,

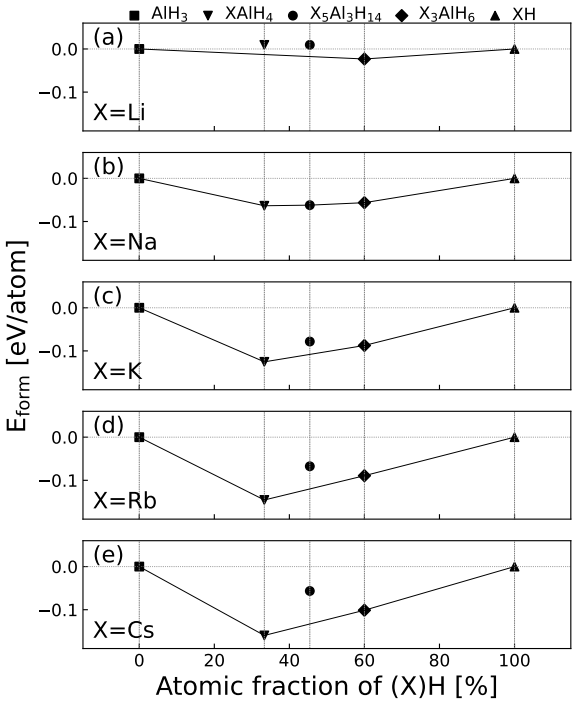

Figure 2: Phase diagrams for crystal group Li-Al-H, Na-Al-H, K-Al-H, Rb-Al-H and Cs-Al-H.

which makes us base the structures on $Na_5Al_3H_{14}$. Therefore these crystals do not necessarily have the symmetry with the lowest energy and thus the most stable configuration. In other words the crystal might have ended up in local energy minimum instead of a global energy minimum during the relaxation. The phase diagram of the Li-B-H category crystals is shown in Figure 3 and the formation energies in Table 5. From those, it is clear that only $LiBH_4$ passes the stability criterium. However, it may be too stable in the sense that the extraction of hydrogen could possibly require too much energy. As stated in section II., the verification of this is out of the scope of this study so a definitive conclusion can not be made.

In conclusion, from the available indicators and chosen crystals in this study, the most suitable ternary hydrides are found to be Li_3AlH_6 and $LiBH_4$. Their properties are listed once again in table 4. From this it is clear that Li_3AlH_6 is preferred when the emphasis is on the crystal having a low formation energy, but $LiBH_4$ is when focusing on maximizing the H_2 density and weight percentage, regardless of formation energy.

IV. Summary

To summarize, using first-principles calculations with a minimum precision of 3 mRy/au in forces and 3 kbar for any component of the stress tensor, numerous ternary hydrides were tested. Some criteria for the selection of useful candidates were established, regarding stability, the volumetric H_2 density and weight

Crystal	# Atoms	Spacegroup	H_2 density [$Å^{-3}$]	Weigth percentage [%]	Pressure [atm]
AlH_3[19]	64	F d -3 m	0.0322	10.08	1286
Li_3AlH_6[20]	60	P -3	0.0343	11.23	1370
$Li_5Al_3H_{14}$*[21]	44	P 4/m n c	0.0375	10.87	1498
$LiAlH_4$[22]	24	P 2/c	0.0373	10.62	1489
LiH[23]	8	F m -3 m	0.031	12.68	1239
Na_3AlH_6[24]	20	P 21/c	0.026	5.93	1039
$Na_5Al_3H_{14}$[21]	44	P 4/m n c	0.0296	6.72	1183
$NaAlH_4$[25]	24	I 41/a	0.0286	7.47	1143
NaH[26]	8	F m -3 m	0.0177	4.2	707
K_3AlH_6[27]	20	P 21/c	0.0192	4.02	767
$K_5Al_3H_{14}$*[21]	44	P 4/m n c	0.0232	4.86	926
$KAlH_4$[28]	24	P n m a	0.0218	5.75	871
KH[29]	2	F m -3 m	0.0109	2.51	434
Rb_3AlH_6*[24]	20	P 21/c	0.0171	2.09	682
$Rb_5Al_3H_{14}$*[21]	44	P 4/m n c	0.0206	2.7	822
$RbAlH_4$[30]	24	P n m a	0.0186	3.46	743
RbH[31]	2	F m -3 m	0.009	1.17	361
Cs_3AlH_6[32]	40	P m -3 m	0.015	1.4	601
$Cs_5Al_3H_{14}$*[21]	44	P 4/m n c	0.0184	1.86	734
$CsAlH_4$[33]	24	I 41/a m d	0.0169	2.46	674
CsH[34]	8	F m -3 m	0.0075	0.75	301
BH_3[35]	16	P 21/c	0.0297	21.86	1188
Li_3BH_6[36]	20	P 1	0.0315	16.05	1258
$Li_5B_3H_{14}$*[21]	44	P 4/m n c	0.0511	17.37	2039
$LiBH_4$[37]	24	P n m a	0.037	18.51	1479

Table 2: Fundamental data of K, Li, Cs, Na category crystals based on the vc-relaxed output files, made with our code on GitHub. Note that the shown pressure is the ideal gas pressure equivalent. Structures that were not readily available on any of the known databases are assigned an asterisk. The CIF files of those structures were created from the Na equivalent by replacing the Na atoms with the relevant element related to the chemical formula.

E_{form} [eV/atom]	$XAlH_4$	$X_5Al_3H_{14}$	X_3AlH_6
X=Li	0.00940	0.00955	-0.02322
X=Na	-0.06348	-0.06207	-0.05635
X=K	-0.12535	-0.07825	-0.08740
X=Rb	-0.14559	-0.06746	-0.08929
X=Cs	-0.15965	-0.05658	-0.10117

Table 3: Formation energies [eV/atom] in phase diagrams in Figure 2. The formation energy is calculated by $E_{\text{form}} = E_{\text{tot}} - n_{\text{AlH}_3} \cdot E_{\text{tot,AlH}_3} - n_{\text{XH}} \cdot E_{\text{tot,XH}}$, where n stands for the amount of times that crystal fits into the composite crystal.

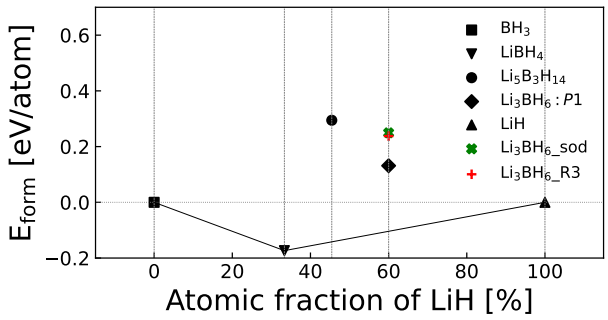

Figure 3: Phase diagram with respect to BH_3-LiH. Different symmetries ([24] (sodium equivalent) and [38] ($R\overline{3}$)) were tested for Li_3BH_6 in search of a stable form, but [36] (P1) gave the least unstable result.

percentage. For the first, phase diagrams (formation energies) were used as an indicator. Combining this with an investigation of the others, we were able to point out two potential candidates for hydrogen storage. These candidates are Li_3AlH_6 and $LiBH_4$.

Note that this study is based on rather simple criteria, making our methods very efficient, but also very limited for making conclusions. The biggest weakness is in the unknown reaction paths, but the proposed candidates could still be very interesting for further research that is more dedicated on doing in-depth studies of a lower number of crystals. Such a study could also allow the binary hydrides to be considered.

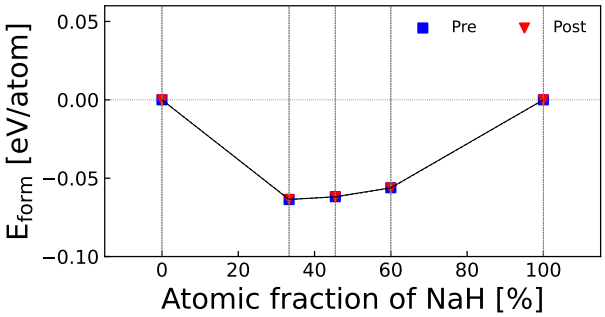

Figure 4: The AlH3-NaH phase diagram before and after structure relaxation. There is not much difference between the two.

Appendix

Diagrams before and after relaxation

In addition, as an example, we compared the formation energies of the crystals in the group Na-Al-H before and after structure relaxation. This is shown in figure 4. Its results show that there was not much difference between the two. However, this does not discard relaxation as a vital step in our workflow. For starters, this being the case for the Na-Al-H category crystals does not prove other crystals also showing this behaviour. Second, leaving out the optimization might intuitively lead to distorted H_2 densities, because of the change in volume. For completeness, the total energies and formation energies before and after optimization of the Na-Al-H category crystals are shown in table 7 and table 8 respectively.

Acknowledgment

The calculations presented above were performed using computer resources within the Aalto University School of Science "Science-IT" project as well as the HPC-UGent and HPC-UAntwerp Tier-2 Infrastructure, which are both part of the VSC.

Conflict of Interest

The authors declare no conflict of interest.

Crystal	H_2 density [$Å^{-3}$]	Weight percentage	Equiv. pressure [atm]	E_{form} [eV/atom]
Li_3AlH_6	0.034	11.23	1370	-0.02322
$LiBH_4$	0.037	18.51	1479	-0.17337

Table 4: Relevant properties most suitable crystals

$LiBH_4$ -0.17337	$Li_5B_3H_{14}$ 0.29451	Li_3BH_6 0.13135
Li_3BH_6_R3 0.23768	Li_3BH_6_sod 0.24939	

Table 5: Formation energies [eV/atom] used in Figure 3.

References

[1] idealhy.eu - liquid hydrogen outline. https://www.idealhy.eu/index.php?page=lh2_outline. (Accessed on 12/09/2023).

[2] Bradley D. Fahlman. *Metals*, pages 171–261. Springer Netherlands, Dordrecht, 2018. ISBN 978-94-024-1255-0. doi: 10.1007/978-94-024-1255-0_3. URL https://doi.org/10.1007/978-94-024-1255-0_3.

[3] Evangelos I. Gkanas. *Metal hydrides: Modeling of metal hydrides to be operated in a fuel cell*, page 67–90. January 2018. doi: 10.1016/b978-0-12-813128-2.00005-x. URL https://doi.org/10.1016/b978-0-12-813128-2.00005-x.

[4] Stefaan Cottenier. Crystals for hydrogen storage. Technical report.

[5] P. Hohenberg and W. Kohn. Inhomogeneous electron gas. *Physical Review*, 136(3B):B864–B871, November 1964. ISSN 0031-899X. doi: 10.1103/physrev.136.b864. URL http://dx.doi.org/10.1103/PhysRev.136.B864.

[6] W. Kohn and L. J. Sham. Self-consistent equations including exchange and correlation effects. *Physical Review*, 140(4A):A1133–A1138, November 1965. ISSN 0031-899X. doi: 10.1103/physrev.140.a1133. URL http://dx.doi.org/10.1103/PhysRev.140.A1133.

[7] Paolo Giannozzi, Stefano Baroni, Nicola Bonini, Matteo Calandra, Roberto Car, Carlo Cavazzoni, Davide Ceresoli, Guido L Chiarotti, Matteo Cococcioni, Ismaila Dabo, Andrea Dal Corso, Stefano de Gironcoli, Stefano Fabris, Guido Fratesi, Ralph Gebauer, Uwe Gerstmann, Christos Gougoussis, Anton Kokalj, Michele Lazzeri, Layla Martin-Samos, Nicola Marzari, Francesco Mauri, Riccardo Mazzarello, Stefano Paolini, Alfredo Pasquarello, Lorenzo Paulatto, Carlo Sbraccia, Sandro Scandolo, Gabriele Sclauzero, Ari P Seitsonen, Alexander Smogunov, Paolo Umari, and Renata M Wentzcovitch. Quantum espresso: a modular and open-source software project for quantum simulations of materials. *Journal of Physics: Condensed Matter*, 21(39):395502, September 2009. ISSN 1361-648X. doi: 10.1088/0953-8984/21/39/395502. URL http://dx.doi.org/10.1088/0953-8984/21/39/395502.

[8] P Giannozzi, O Andreussi, T Brumme, O Bunau, M Buongiorno Nardelli, M Calandra, R Car, C Cavazzoni, D Ceresoli, M Cococcioni, N Colonna, I Carnimeo, A Dal Corso, S de Gironcoli, P Delugas, R A DiStasio, A Ferretti, A Floris, G Fratesi, G Fugallo, R Gebauer, U Gerstmann, F Giustino, T Gorni, J Jia, M Kawamura, H-Y Ko, A Kokalj, E Küçükbenli, M Lazzeri, M Marsili, N Marzari, F Mauri, N L Nguyen, H-V Nguyen, A Otero-de-la Roza, L Paulatto, S Poncé, D Rocca, R Sabatini, B Santra, M Schlipf, A P Seitsonen, A Smogunov, I Timrov, T Thonhauser, P Umari, N Vast, X Wu, and S Baroni. Advanced capabilities for materials modelling with quantum espresso. *Journal of Physics: Condensed Matter*, 29(46):465901, October 2017. ISSN 1361-648X. doi: 10.1088/1361-648x/aa8f79. URL http://dx.doi.org/10.1088/1361-648X/aa8f79.

[9] John P. Perdew, Kieron Burke, and Matthias Ernzerhof. Generalized gradient approximation made simple. *Physical Review Letters*, 77 (18):3865–3868, October 1996. doi: 10.1103/physrevlett.77.3865. URL https://doi.org/10.1103/physrevlett.77.3865.

[10] Gianluca Prandini, Antimo Marrazzo, Ivano E Castelli, Nicolas Mounet, and Nicola Marzari. Precision and efficiency in solid-state pseudopotential calculations. *npj Computational Materials*, 4(1):72, 2018. ISSN 2057-3960. doi: 10.1038/s41524-018-0127-2. URL https://www.nature.com/articles/s41524-018-0127-2. http://materialscloud.org/sssp.

[11] Ask Hjorth Larsen, Jens Jørgen Mortensen, Jakob Blomqvist, Ivano E Castelli, Rune Christensen, Marcin Dułak, Jesper Friis, Michael N Groves, Bjørk Hammer, Cory Hargus, Eric D Hermes, Paul C Jennings, Peter Bjerre Jensen, James Kermode, John R Kitchin, Esben Leonhard Kolsbjerg, Joseph Kubal, Kristen Kaasbjerg, Steen Lysgaard, Jón Bergmann Maronsson, Tristan Maxson, Thomas Olsen, Lars Pastewka, Andrew Peterson, Carsten Rostgaard, Jakob Schiøtz, Ole Schütt, Mikkel Strange, Kristian S Thygesen, Tejs Vegge, Lasse Vilhelmsen, Michael Walter, Zhenhua Zeng, and Karsten W Jacobsen. The atomic simulation environment—a python library for working with atoms. *Journal of Physics: Condensed Matter*, 29(27): 273002, 2017. URL http://stacks.iop.org/0953-8984/29/i=27/a=273002.

Crystal	Degrees of freedom	# Atom number	H2 pairs per volume [$\AA^{-3}$]	Pressure [atm]
AlH_3	1 + 1	64	0.03332	1354.973
$NaAlH_4$	2 + 3	24	0.02982	1218.516
$Na_5Al_3H_{14}$	2 + 7	44	0.03080	1258.715
Na_3AlH_6	4 + 12	20	0.02709	1107.229
NaH	1 + 0	8	0,01839	751.6966

Table 6: Geometrical degrees of freedom, number of atoms, H_2 density and pressure of the Na type crystals.

	total E [Ry]	total E after opt [Ry]
AlH_3	-172.02145099	-172.02376572
$NaAlH_4$	-279.14766133	-279.14800187
$Na_5Al_3H_{14}$	-1223.63600254	-1223.64281612
Na_3AlH_6	-665.33845447	-665.33862262
NaH	-386.16160256	-386.16264830

Table 7: Total energies before and after optimization of the Na-Al-H category crystals

	E_{init}[eV/atom]	E_{relax} [eV/atom]
AlH_3	0	0
$NaAlH_4$	-0,06364545	-0,06346385
$Na_5Al_3H_{14}$	-0,06178818	-0,06204824
Na_3AlH_6	-0,05610553	-0,05632537
NaH	0	0

Table 8: Formation energies before and after optimization of the Na-Al-H category crystals

[12] S. R. Bahn and K. W. Jacobsen. An object-oriented scripting interface to a legacy electronic structure code. *Comput. Sci. Eng.*, 4(3):56–66, MAY-JUN 2002. ISSN 1521-9615. doi: 10.1109/5992.998641.

[13] Shyue Ping Ong, William Davidson Richards, Anubhav Jain, Geoffroy Hautier, Michael Kocher, Shreyas Cholia, Dan Gunter, Vincent L Chevrier, Kristin A Persson, and Gerbrand Ceder. Python materials genomics (pymatgen): A robust, open-source python library for materials analysis. *Computational Materials Science*, 68:314–319, 2013.

[14] Mois Ilia Aroyo, Juan Manuel Perez-Mato, Cesar Capillas, Eli Kroumova, Svetoslav Ivantchev, Gotzon Madariaga, Asen Kirov, and Hans Wondratschek. Bilbao crystallographic server: I. databases and crystallographic computing programs. *Zeitschrift für Kristallographie - Crystalline Materials*, 221(1):15–27, January 2006. ISSN 2194-4946. doi: 10.1524/zkri.2006.221.1.15. URL http://dx.doi.org/10.1524/zkri.2006.221.1.15.

[15] Mois I. Aroyo, Asen Kirov, Cesar Capillas, J. M. Perez-Mato, and Hans Wondratschek. Bilbao crystallographic server. ii. representations of crystallographic point groups and space groups. *Acta Crystallographica Section A Foundations of Crystallography*, 62(2):115–128, March 2006. ISSN 0108-7673. doi: 10.1107/s0108767305040286. URL http://dx.doi.org/10.1107/S0108767305040286.

[16] Mois I Aroyo, Juan Manuel Perez-Mato, Danel Orobengoa, EMRE Tasci, Gemma de la Flor, and Asel Kirov. Crystallography online: Bilbao crystallographic server. *Bulg. Chem. Commun*, 43(2): 183–197, 2011.

[17] Torbjörn Björkman. Cif2cell: Generating geometries for electronic structure programs. *Computer Physics Communications*, 182(5):1183–1186, May 2011. ISSN 0010-4655. doi: 10.1016/j.cpc.2011.01.013. URL http://dx.doi.org/10.1016/j.cpc.2011.01.013.

[18] Anubhav Jain, Shyue Ping Ong, Geoffroy Hautier, Wei Chen, William Davidson Richards, Stephen Dacek, Shreyas Cholia, Dan Gunter, David Skinner, Gerbrand Ceder, and Kristin A. Persson. Commentary: The Materials Project: A materials genome approach to accelerating materials innovation. *APL Materials*, 1(1):011002, 07 2013. ISSN 2166-532X. doi: 10.1063/1.4812323. URL https://doi.org/10.1063/1.4812323.

[19] mp-1106356: Alh3 (cubic, fd-3m, 227). https://next-gen.materialsproject.org/materials/mp-1106356, . (Accessed on 12/09/2023).

[20] mp-31096: Li3alh6 (trigonal, r-3, 148). https://next-gen.materialsproject.org/materials/mp-31096?formula=Li3AlH6, . (Accessed on 12/09/2023).

[21] mp-24822: Na5al3h14 (tetragonal, p4/mnc, 128). https://next-gen.materialsproject.org/materials/mp-24822, . (Accessed on 12/09/2023).

[22] mp-1180547: Lialh4 (monoclinic, c2/c, 15). https://next-gen.materialsproject.org/materials/mp-1180547?formula=LiAlH4, . (Accessed on 12/09/2023).

[23] mp-23703: Lih (cubic, fm-3m, 225). https://next-gen.materialsproject.org/materials/mp-23703?formula=LiH, . (Accessed on 12/09/2023).

[24] mp-23705: Na3alh6 (monoclinic, p2_1/c, 14). https://next-gen.materialsproject.org/materials/mp-23705, . (Accessed on 12/09/2023).

[25] mp-23704: Naalh4 (tetragonal, i4_1/a, 88). https://next-gen.materialsproject.org/materials/mp-23704, . (Accessed on 12/09/2023).

[26] mp-23870: Nah (cubic, fm-3m, 225). https://next-gen.materialsproject.org/materials/mp-23870, . (Accessed on 12/09/2023).

[27] mp-24034: K3alh6 (monoclinic, p2_1/c, 14). https://next-gen.materialsproject.org/materials/mp-24034?formula=K3AlH6, . (Accessed on 12/09/2023).

[28] mp-31097: Kalh4 (orthorhombic, pnma, 62). https://next-gen.materialsproject.org/materials/mp-31097?formula=KAlH4, . (Accessed on 12/09/2023).

[29] mp-24084: Kh (cubic, fm-3m, 225). https://next-gen.materialsproject.org/materials/mp-24084?formula=KH, . (Accessed on 12/09/2023).

[30] mp-1209241: Rbalh4 (orthorhombic, pnma, 62). https://next-gen.materialsproject.org/materials/mp-1209241?chemsys=Rb-Al-H, . (Accessed on 12/09/2023).

[31] mp-24721: Rbh (cubic, fm-3m, 225). https://next-gen.materialsproject.org/materials/mp-24721, . (Accessed on 12/09/2023).

[32] Cs3alh6. https://oqmd.org/materials/entry/1374287. (Accessed on 12/09/2023).

[33] Csalh4. https://oqmd.org/materials/entry/1371930. (Accessed on 12/09/2023).

[34] mp-1057286: Csh (cubic, fm-3m, 225). https://next-gen.materialsproject.org/materials/mp-1057286?formula=CsH, . (Accessed on 12/09/2023).

[35] mp-634117: Bh3 (monoclinic, p2_1/c, 14). https://next-gen.materialsproject.org/materials/mp-634117?formula=BH3. (Accessed on 12/09/2023).

[36] mp-1180683: Li3bh6 (triclinic, p1, 1). https://next-gen.materialsproject.org/materials/mp-1180683?chemsys=Li-B-H, . (Accessed on 12/09/2023).

[37] mp-1192133: Libh4 (orthorhombic, pnma, 62). https://next-gen.materialsproject.org/materials/mp-1192133?formula=LiBH4, . (Accessed on 12/09/2023).

[38] mp-1180675: Li3bh6 (trigonal, r-3, 148). https://next-gen.materialsproject.org/materials/mp-1180675?formula=Li3BH6, . (Accessed on 12/10/2023).